in *Biological Effects of Microwave Radiation*, vol. 1. New York: Plenum, 1960, pp. 153–176.
[3] A. R. Shapiro, R. F. Lutomirski, and H. T. Yura, "Induced fields and heating within a cranial structure irradiated by an electromagnetic plane wave," *IEEE Trans. Microwave Theory Tech.* (*Special Issue on Biological Effects of Microwaves*), vol. MTT-19, pp. 187–196, Feb. 1971.
[4] H. N. Kritikos and H. P. Schwan, "Hot spots generated in conducting spheres by electromagnetic waves and biological implications," *IEEE Trans. Biomed. Eng.*, vol. BME-19, pp. 53–58, Jan. 1972.
[5] J. C. Lin, A. W. Guy, and C. C. Johnson, "Power deposition in a spherical model of man exposed to 1–20 MHz electromagnetic fields," *IEEE Trans. Microwave Theory Tech.*, vol. MTT-21, pp. 791–797, Dec. 1973.
[6] W. T. Joines and R. J. Spiegel, "Resonance absorption of microwaves by the human skull," *IEEE Trans. Biomed. Eng.*, vol. BME-21, pp. 46–48, Jan. 1974.
[7] A. W. Guy, "Analysis of electromagnetic field induced in biological tissue by thermographic studies on equivalent phantom models," *IEEE Trans. Microwave Theory Tech.*, vol. MTT-19, pp. 205–214, Feb. 1971.
[8] C. M. Weil, "Absorption characteristics of multilayered sphere models exposed to UHF/microwave radiation," *IEEE Trans. Biomed. Eng.*, vol. BME-22, pp. 468–476, Nov. 1975.
[9] H. N. Kritikos and H. P. Schwan, "The distribution of heating potential inside lossy spheres," *IEEE Trans. Biomed. Eng.*, vol. BME-22, pp. 457–463, Nov. 1975.
[10] C. C. Johnson, C. H. Durney, and H. Massoudi, "Electromagnetic power absorption in anisotropic tissue media," *IEEE Trans. Microwave Theory Tech.*, vol. MTT-23, pp. 529–532, June 1975.
[11] C. H. Durney, C. C. Johnson, and H. Massoudi, "Long-wavelength analysis of planewave irradiation of a prolate spheroid model of man," *IEEE Trans. Microwave Theory Tech.*, vol. MTT-23, pp. 246–253, Feb. 1975.
[12] C. C. Johnson, C. H. Durney, and H. Massoudi, "Long-wavelength electromagnetic power absorption in prolate spheroidal models of man and animals," *IEEE Trans. Microwave Theory Tech.*, vol. MTT-23, pp. 739–747, Sept. 1975.
[13] S. J. Allen, W. D. Hurt, J. H. Krupp, J. A. Ratliff, C. H. Durney, and C. C. Johnson, "Measurement of radio-frequency power absorption in monkeys, monkey phantoms, and human phantoms exposed to 10–50 MHz fields," in *Proc. 1975 Annu. USNC/URSI Meeting* (Boulder, CO), Oct. 1975, p. 200.
[14] O. P. Gandhi, "Frequency and orientation effects on whole animal absorption of electromagnetic waves," *IEEE Trans. Biomed. Eng.*, vol. BME-22, pp. 536–542, Nov. 1975.
[15] H. Massoudi, C. H. Durney, and C. C. Johnson, "Long-wavelength analysis of plane wave irradiation of an ellipsoidal model of man," this issue, pp. 41–46.
[16] H. P. Schwann, "Electrical properties of tissues and cells," *Advan. Biol. Med. Phys.*, vol. 5, pp. 147–209, 1957.
[17] *Collier's Encyclopedia*, vol. 19.
[18] *Encyclopedia Britannica*, vol. 7.
[19] H. Dreyfuss, *The Measure of Man, Human Factors in Design*, Whitney Library of Design, New York, 1967.
[20] S. J. Allen, W. D. Hurt, J. H. Krupp, J. A. Ratliff, C. H. Durney, and C. C. Johnson, "Measurement of radio frequency power absorption in monkeys, monkey phantoms, and human phantoms exposed to 10–50 MHz fields," Report SAM-TR-76-5, USAF School of Aerospace Medicine, Aerospace Medical Division (AFSC), Brooks Air Force Base, TX 78235.

Short Papers

New Method for Computing the Resonant Frequencies of Dielectric Resonators

TATSUO ITOH, SENIOR MEMBER, IEEE, AND RONALD S. RUDOKAS, STUDENT MEMBER, IEEE

***Abstract*—A new method is developed for accurately predicting resonant frequencies of dielectric resonators used in microwave circuits. By introducing an appropriate approximation in the field distribution outside the resonator, an analytical formulation becomes possible. Two coupled eigenvalue equations thus derived are subsequently solved by a numerical method. The accuracy of the results computed by the present method is demonstrated by comparison with previously published data.**

I. Introduction

Dielectric resonators made of high permittivity material have found practical applications in microwave circuits due mainly to their high-Q values. The dominant $TE_{01\delta}^{\circ}$ mode in the low-profile cylindrical resonators [Fig. 1(a)] has traditionally been analyzed by using the so-called magnetic wall model, in which the cylindrical surface containing the circumference of the resonator is replaced with a fictitious open-circuit boundary (magnetic wall) [1]. Recently, Konishi *et al.* [2] reported a more accurate method based on the variational procedure for computing the resonant frequency of $TE_{01\delta}^{\circ}$ modes. Their predicted resonant frequencies agree with experimental data within 1 percent [2]. On the other hand, the magnetic wall method typically gives rise to numerical values smaller than the experimental by about 10 percent.

The method reported by Garault and Guillon [4] is also capable of predicting the resonant frequency with less than 1 percent error. In their method, successive application of imperfect magnetic wall conditions on side and end walls results

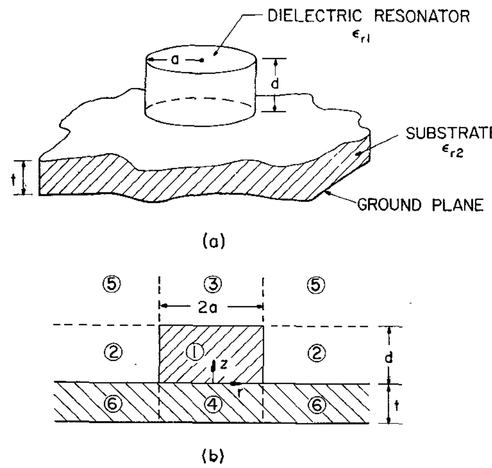

Fig. 1. (a) Dielectric resonator. (b) Side view of dielectric resonator.

Manuscript received April 1, 1976; revised June 28, 1976. This work was supported in part by U.S. Army Research Grant DAHC04-74-G0113 and in part by Joint Services Electronics Program DAAB07-72-C-0259.

T. Itoh was with the Department of Electrical Engineering and the Coordinated Science Laboratory, University of Illinois, Champaign/Urbana, IL 61801. He is now with the Stanford Research Institute, Menlo Park, CA 94025.
R. S. Rudokas was with the Department of Electrical Engineering and the Coordinated Science Laboratory, University of Illinois, Champaign/Urbana, IL 61801. He is now with the Electromagnetic Systems Laboratory Inc., Sunnyvale, CA 94086.

in the dielectric resonator of effective height and radius. From this process, an accurate resonant frequency is obtained.

In this short paper, a simple numerical procedure is reported for predicting the resonant frequencies of $TE_{01\delta}^{\circ}$ modes in cylindrical dielectric resonators. The method is based on the semianalytical technique originally developed by Marcatili [3] for analyzing the propagation characteristics of a rectangular dielectric waveguide, and extended here to apply to the three-dimensional cylindrical resonator structure. Although slight modifications of the formulation make it possible to analyze rectangular resonators [1] as well, such extensions are not included here.

II. Method of Analysis

In Fig. 1(a), a typical dielectric resonator is placed on a dielectric substrate which is in turn backed by a ground plane. The relative dielectric constant ε_{r1} of the resonator is much higher than that of the substrate ε_{r2}. When $\varepsilon_{r2} = 1$ and the substrate thickness t becomes infinity, the structure represents the resonator in free space as analyzed in [1] and [2].

The major difficulty in the analysis of dielectric resonators lies in the fact that the structure as shown in Fig. 1 does not belong to a separable geometry. The rigorous analysis requires quite complicated formulations. However, it is possible to introduce a simplification which leads to a pair of conventional eigenvalue equations. This simplification arises from observing that in a high-Q resonator most of the electromagnetic energy is stored in region 1 [see Fig. 1(b)] and the field decays exponentially in regions 2–4. A small amount of energy is in 2–4 and even less is in regions 5 and 6. Therefore, only a small error is introduced in the calculation of resonant characteristics if one ignores the field in 5 and 6 and removes the requirement of matching the field between regions 2 and 5, 6, etc. It is now necessary to match the field only on the boundary surfaces of region 1.

For TE modes which have no circumferential variation, the H_z field in each region may be written as

$$H_z = \begin{cases} A_1 \sin \beta(z - z_0) J_0(hr) & \text{region 1} \quad (1a) \\ A_2 \sin \beta(z - z_0) K_0(pr) & \text{region 2} \quad (1b) \\ A_3 \exp\left[-\gamma(z - d)\right] J_0(hr) & \text{region 3} \quad (1c) \\ A_4 \sinh\left[\xi(z + t)\right] J_0(hr) & \text{region 4} \quad (1d) \end{cases}$$

where

$$\beta^2 = \varepsilon_{r1} k_0{}^2 - h^2 = k_0{}^2 + p^2$$
$$\gamma^2 = h^2 - k_0{}^2 \quad \xi^2 = h^2 - \varepsilon_{r2} k_0{}^2$$
$$k_0 = \omega_0 \sqrt{\varepsilon_0 \mu_0} \tag{2}$$

and z_0, A_1, A_2, A_3, and A_4 are constants to be determined. J_0 and K_0 are the Bessel and the modified Hankel functions of order zero. ω_0 is the angular resonant frequency. All the field components can easily be derived from (1). Note that $E_z = E_r = H_\theta = 0$ for TE modes with no circumferential field variation.

The next task is to apply the continuity conditions on H_z and E_θ at $r = a$, $0 < z < d$, and E_θ and H_r at $z = 0$ and d, $0 < r < a$. When this is done, A_1–A_4 and z_0 can be eliminated to yield two coupled eigenvalue equations

$$\begin{cases} \dfrac{J_0'(ha)}{hJ_0(ha)} + \dfrac{K_0'(pa)}{pK_0(pa)} = 0 & (3a) \\ \beta d = q\pi + \tan^{-1}\left(\dfrac{\gamma}{\beta}\right) & \\ \qquad + \tan^{-1}\left(\dfrac{\xi}{\beta} \coth \xi t\right), \quad q = 0,1,2,\cdots & (3b) \end{cases}$$

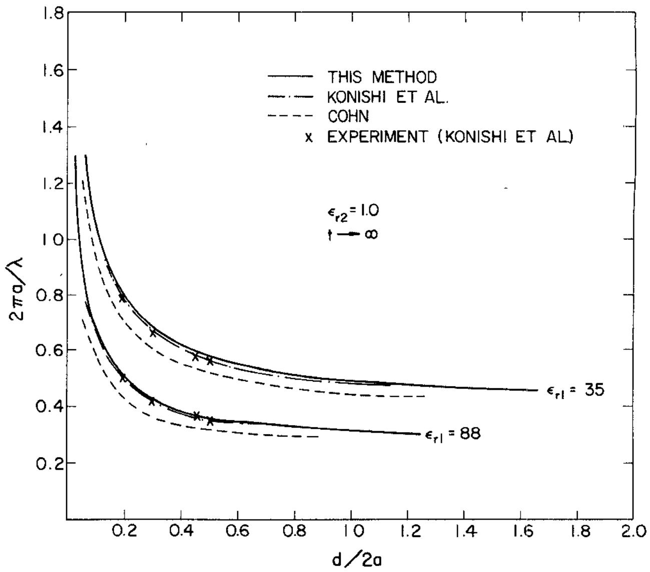

Fig. 2. Numerical results of the resonant frequency.

where the principal branches are to be taken for the arctangent functions. The primes in (3a) indicate differentiation with respect to arguments. Equations (3a) and (3b) together with (2) are then solved for the resonant frequency ω_0. It should be noted that, in the magnetic wall model (3a) is replaced with

$$J_0(ha) = 0. \tag{4}$$

This equation is the consequence of the imposition of the artificial open boundary condition on the cylindrical surface. This oversimplification caused the predicted resonant frequencies in [1] to be substantially lower than the experimental data.

Before concluding this section, let us discuss the designation of the mode index. For a given k_0, (3a) has a finite number of roots which correspond to different radial field distributions. The orders of these roots are numbered with the index m starting from 1. On the other hand, the field variation in the axial (z) direction is governed by the index q. In the circumferential direction, the field does not vary and hence the index takes only the value zero. The resonant modes are now designated as TE_{0mq}, and the dominant mode TE_{010} is often referred to in the literature [2] as $TE_{01\delta}^{\circ}$.

III. Numerical Results

The resonant frequency of the dominant mode in the dielectric resonator placed in free space has been computed. For this case, $\varepsilon_{r2} = 1$ and $t \to \infty$, so that (3b) becomes

$$\beta \tan\left(\frac{\beta d}{2}\right) = \gamma \tag{5}$$

for $q = 0$.

In Fig. 2, numerical results for the resonators with the structural parameters identical to those in [2] are plotted. The resonant frequencies predicted by the present method agree favorably with the experimental data and results computed by Konishi *et al.* [2], while those derived by the magnetic wall model are considerably lower. It should also be noted that the agreement between the present and Konishi's methods is better for $\varepsilon_{r1} = 88$ than $\varepsilon_{r1} = 35$. This is expected, since the basic assumption of the present method becomes less valid for resonators with lower dielectric constants and hence lower Q.

IV. Conclusions

A new method has been presented for computing the resonant frequencies of cylindrical dielectric resonators.

Although the method by Konishi *et al.* [2] is more accurate, particularly for resonators with lower dielectric constants, their method is considerably more complicated than the present one. The method in [4] is also more complicated than the present one. With almost the same order of simplicity in formulation and computational labor as the magnetic wall model [1], the present method provides results in close agreement with data reported in [2].

Acknowledgment

The authors wish to thank Dr. A. Jamieson of the New Zealand Post Office, who is on leave at the University of Illinois, for his many useful comments.

References

[1] S. B. Cohn, "Microwave bandpass filters containing high-Q dielectric resonators," *IEEE Trans. Microwave Theory Tech.*, vol. MTT-16, pp. 218–299, Apr. 1968.
[2] Y. Konishi, N. Hoshino, and Y. Utsumi, "Resonant frequency of a $TE_{01\delta}^{0}$ dielectric resonator," *IEEE Trans. Microwave Theory Tech.*, vol. MTT-24, pp. 112–114, Feb. 1976.
[3] E. A. J. Marcatili, "Dielectric rectangular waveguide and directional coupler for integrated optics," *Bell Syst. Tech. J.*, vol. 48, pp. 2071–2102, Sept. 1969.
[4] Y. Garault and P. Guillon, "Best approximation for design of natural resonance frequencies of microwave dielectric disc resonants," *Electronics Letters*, vol. 10, pp. 505–507, Nov. 28, 1974.

Conversion Loss Limitations on Schottky-Barrier Mixers

MALCOLM McCOLL

***Abstract*—A new set of criteria involving diode area, material parameters, and temperature is introduced for the Schottky-barrier mixer diode that must be considered if its usage is to be extended to the submillimeter wavelength region or cryogenically cooled to reduce the noise contribution of the mixer. It has been well established that, in order to reduce the parasitic loss as the frequency is increased, it is necessary to reduce the area of the diode. What has not been analyzed heretofore is the effect that a reduction in diode area can have on the intrinsic conversion loss L_0 of the diode resulting from its nonlinear resistance. This analysis focuses on the competing requirements of impedance matching the diode to its imbedding circuit and the finite dynamic range of the nonlinear resistance. As a result, L_0 can increase rapidly as the area is reduced. Results are first expressed in terms of dimensionless parameters, and then some respresentative examples are investigated in detail. The following conclusions are drawn: a large Richardson constant extends the usefulness of the diode to smaller diameters, and hence, shorter wavelengths; cooling a thermionic emitting diode can have a very detrimental effect on L_0; impedance mismatching is found, in general, to be a necessity for minimum conversion loss; and large barrier heights are desirable for efficient tunnel emitter converters.**

I. Introduction

The metal–semiconductor contact, or Schottky-barrier diode, has a long history of utilization as a mixer element [1], [2]. Its use has progressed to higher and higher frequencies, with the highest frequency recently being demonstrated by Fetterman *et al.*, who observed mixing at 3 THz with a GaAs Schottky diode [3]. For efficient operation at submillimeter wavelengths, many previously accepted tenets applicable to the design of microwave Schottky diodes must be reexamined.

Mixer conversion loss L_c, defined as the ratio of available power from the RF source to the power absorbed in the IF load, can be expressed in the form

$$L_c = L_0 L_p. \tag{1}$$

The intrinsic conversion loss L_0 is the loss arising from the conversion process within the nonlinear resistance of the diode and includes the impedance mismatch losses at the RF and IF ports. The parasitic loss L_p is the loss associated with the parasitic elements of the diode, the junction capacitance, and spreading resistance. Defined as the ratio of total power absorbed by the impedance R_m of the nonlinear resistance at the signal frequency, L_p is given by [4]

$$L_p = 1 + R_s/R_m + \omega_1^2 C^2 R_m R_s \tag{2}$$

where ω_1 is the signal angular frequency and C is the junction capacitance. The spreading resistance R_s is the resistance resulting from constriction of current flow in the semiconductor near the contact and is in series with the parallel elements C and R_m. Since $C \propto d^2$ and $R_s \propto d^{-1}$, where d is the diameter of the junction, (2) indicates that d should be reduced as the frequency of interest is increased. With the development of electron beam fabrication techniques [5], [6], the ability to produce Schottky barriers with dimensions of the order of a few hundred angstroms is imminent. However, the effect of a reduction in area on the intrinsic conversion loss L_0 must also be evaluated to determine overall mixer performance. This consideration is the central topic of this short paper.[1]

The dependence of L_0 on area originates in the impedance requirements the circuit places on the device. In order for the diode, driven by a local oscillator (LO), to couple most efficiently to a circuit with a specified impedance, it must pass approximately the same current, independent of the junction size. Hence reducing the size of the diode increases the current density through the device and, as a consequence, the dc bias voltage V_0 must be increased. Increasing V_0 limits the useful amplitude of the LO voltage V_1 because the current–voltage (I–V) characteristic of the junction in the forward direction is only nonlinear for applied voltages less than the barrier height potential V_B of the metal–semiconductor interface. Since $V_0 + V_1 \leq V_B$, decreasing the area serves to limit V_1, and consequently may increase L_0.

Because of the inverse relationship between the RF impedance of the diode and the bias current, superior results should be obtained for small areas if the Richardson constant of the semiconductor and the impedance of the circuit are large. The much larger Richardson constant of silicon extends its usefulness to smaller diameters than gallium arsenide. Moreover, it is predicted that the diode should be operated in an impedance mismatched condition; cooling a thermionic emitting diode can have a very detrimental effect on L_0, and large values of barrier height are desirable for efficient tunnel emitter converters.

From the classical conversion loss equations developed in Section II, specific situations are analyzed in Section III. Optimum coupling between the diode and the circuit is first analyzed. This result is applied to both thermionic emitting n-GaAs and n-Si Schottky diodes operating at 290 and 77 K,

Manuscript received March 22, 1976; revised June 28, 1976.
The author is with the Electronics Research Laboratory, The Aerospace Corporation, El Segundo, CA 90245.

[1] For examples of L_p values with Schottky barriers on GaAs, Si, and Ge for wavelengths extending into the submillimeter, the reader is referred to [7].